27p

COMPARISON OF PRE-LAUNCH AND FLIGHT VIBRATION MEASUREMENTS ON THOR LAUNCH VEHICLES

By S. A. Clevenson and W. B. Tereniak 1963 22 p refs

602 1448 | NASA Langley Research Center, Langley Station, Hampton, Va.

Presented at the 33rd Symposium on Shock, Vibration, and Associated Environments, Washington, D.C., Dec. 3-5, 1963

Washington, D.C.
December 3-5, 1963

COMPARISON OF PRE-LAUNCH AND FLIGHT VIBRATION MEASUREMENTS ON THOR LAUNCH VEHICLES[1]

By S. A. Clevenson[2] and W. B. Tereniak[3]

INTRODUCTION

One of the many obstacles that a spacecraft must overcome in order to operate successfully in space is the severe environment imposed during the launch and powered-flight phases. To assure that the spacecraft is capable of surviving such environments, it is subjected to extensive environmental testing. In order to establish adequate environmental simulation criteria, flight data must be obtained. Flight shock and vibration data were obtained during two suborbital flights of ECHO A-12 in which modified Thor launch vehicles were used (fig. 1). Prior to the launching of the second vehicle, a vibration survey of the forward equipment compartment housing the flight vibration transducers was made while the Thor was on the launch pad at Cape Canaveral.

The purpose of this paper is to present measured flight data and to compare these data with measurements obtained during a vibration survey of the equipment compartment of a Thor launch vehicle. These data will also be compared to pre-flight environmental acceptance test specifications. The paper will be concluded with a discussion of flight data showing the effect of nose fairing shapes.

---

[1]Paper presented at the 33rd Symposium on Shock, Vibration, and Associated Environments, Dec. 3-5, 1963, Washington, D.C.

[2]Aerospace Engineer, Langley Research Center.

[3]Aerospace Engineer, Goddard Space Flight Center.

DISCUSSION

Description of Launch Vehicle

Figure 2 shows a cutaway view of the launch vehicle used for the suborbital firings of the ECHO A-12 passive communications satellite. These vehicles are designated AVT-1 and 2. The main booster was a modified DM-21 Thor missile. Mounted above the Thor forward compartment was the spacecraft equipment compartment to which the spacecraft adapter was secured. The spacecraft, in turn, was secured to the adapter with a marman clamp held together with explosive bolts. Three piezoelectric vibration accelerometers (transducers) were mounted at the base of the adapter on the outer ring stiffener of the equipment compartment (fig. 3). The vibration system incorporated channels 13, A, and C of PDM/FM/FM (pulse duration modulation, frequency modulation, frequency modulation) telemeter to indicate accelerations along the yaw, pitch, and longitudinal axes, respectively. Additional information pertaining to the instrumentation may be found in reference 1.

Overall Vibration Levels

Figure 4 indicates how closely the overall rms vibratory levels measured on AVT-2 compare with those measured on AVT-1. The levels for the accelerations measured on AVT-1 and AVT-2 are given as one curve for the pitch axis and one curve for the yaw axis, since there was less than 10-percent difference in level between the two flights. The accelerations in the longitudinal direction closely agree except for the clipped region of AVT-1. Clipping of instantaneous peaks occurred during the flight time interval of 33 to 43 seconds on AVT-1. Time T is referred to ignition time of the vehicle. During the AVT-1 flight there were two periods of radio-frequency signal dropout where no data were received; AVT-2 experienced no such dropouts. It is significant that

at AVT-2 liftoff (T = 2 seconds) the value of acceleration measured on the longitudinal axis was 2.2 g-rms, whereas at approximately Mach 1 (T = 39 seconds) the acceleration level was 9.4 g-rms. The measured vibration level of 9.4 g-rms is somewhat greater than that indicated by previous measurements made in the forward compartment during flights of the Thor booster. A comparison of AVT-1, AVT-2, and previous Thor flight data - at the main event times - is given in table 1. A sketch showing the transducer locations and comparing the nose shapes of the AVT Thor with previous Thor's is shown in figure 5.

Table 1

Comparison of AVT-1, AVT-2, and Thor Flight Data at Main Event Times

[Vibration level, g-rms]

Event	*AVT-1		*AVT-2		Previous Thor data‡	
	Longitudinal axis	Pitch axis	Longitudinal axis	Pitch axis	Longitudinal axis	Pitch axis
Main engine ignition	1.8	0.93	2.2	0.8	1.7	3.7
Mach 1	8.8**	3.2	9.4	3.0	---	---
Maximum dynamic pressure	3.5	1.6	4.7	1.6	1.7	3.2
Main engine cutoff	.35	.45	.95	.47	---	.5

*AVT low pass output filters at 2.1 kc.

‡Bandwidth unknown.

**Signal clipped and level not considered valid.

Differences in flight-measured vibration levels between AVT and previous Thor flights may be accounted for by differences in transducer location, mass

loading, and stiffness of the mounting structure and by differences in the thrust output of the Thor booster (AVT-1 and AVT-2 had 10 percent greater thrust than previous Thor boosters). In general, the previous low values of measured vibration levels were obtained from transducers located on the central bulkhead in the Thor forward compartment, whereas on AVT-1 and AVT-2 the transducers were located on the inner circumference of the structural attach ring at the top of the spacecraft equipment compartment. (See fig. 3.)

Random Vibrations

As shown in figure 4, the overall rms vibration level begins to build up again at about T = 20 seconds and reaches a peak at T = 39 seconds, at a level of 9.4 g-rms for AVT-2. This buildup in level, which occurs in the transonic region of flight, is attributed to the random excitation caused by aerodynamic buffeting.

Figure 6 shows a power spectral density (PSD) plot for the accelerations in the longitudinal direction using a 20-cps bandwith filter at T = 39 seconds (Mach number $\approx$ 1). It is interesting to note that predominant frequencies measured correspond to frequencies determined from transients occurring at lift-off, main engine cutoff, fairing separation, and spacecraft separation. The high PSD level (0.488 g^2/cps) measured at 1,030 cps is significant. The equivalent g-rms level in the region 940 cps to 1,120 cps is 6.62 g-rms, whereas the overall level at this time was 9.4 g-rms.

Shock or Transient Response

The composite records indicated the vibrations excited by lift-off, MECO, fairing separation, and spacecraft separation. These vibrations are short in duration and relatively high in level. Overall levels measured during fairing

separation and spacecraft separation are beyond the optimum signal range of the measuring channels. These signals are in the nonlinear range of the system and may have been "clipped" by the limiter circuit in the charge amplifier. However, it was felt that a spectral analysis of these data would be enlightening.

A tabulation of the results of the qualitative analysis performed on the vibrations excited by the above-mentioned events of both flights is given in tables 2 and 3. The data were reduced by re-recording a continuous 1-second loop that included the transient vibration, and were then played back into a spectral wave analyzer that employed a 20-cps bandwidth filter. The levels presented are relative, since the time duration of the vibration signal was considerably shorter than the analyzer RC averaging time (1 second) used. The tables summarizing the predominant frequencies indicate that as a result of shocklike excitation certain resonant frequencies are excited. At lift-off these frequencies are excited by both shocklike and acoustic excitations. It is noteworthy that the frequencies are similar in value for these events. This similarity indicates that the high frequencies (greater than 200 cps) are due to a more localized response - that is, from the Thor spacecraft equipment compartment - and are not indicative of the response of the entire vehicle. The previous statement is based on the fact that the mass varies during powered flight and, in turn, varies the vibratory modes of the vehicle.

Figure 7 shows the predominant transient frequencies at lift-off for three Thor vehicles. A narrow band filter was used to obtain the response as a function of time. The upper sketch indicates the transient for the AVT flights at 17 cps. The center sketch (ref. 2) shows the filtered transient for the Thor-Delta vehicle at 16 cps. The bottom sketch (obtained from unpublished data by J. Nagy, GSFC, NASA) shows the filtered transient response for the Thor-Agena

at 18 cps. It may be noted that ground resonance tests by Douglas Aircraft Company have indicated a resonance of the rocket engine on its hydraulic control actuators at about 17 cps. The data show that substantial vibrations at a frequency approximately equal to this ground measured resonant frequency appear in many flights of Thor vehicles.

Vibration Survey of Equipment Compartment

The vibration survey was performed on the fully assembled AVT-2 vehicle prior to fueling on its launch pad at Cape Canaveral. Low-level sinusoidal vibration inputs (15 to 2,000 cps) into the equipment compartment were accomplished by attaching two 25-pound electromagnetic shakers to the nose fairing dummy explosive bolts located 180° apart at station 52.05. Responses to sinusoidal excitations were measured by the flight transducers and by transducers mounted at various external locations on the equipment compartment. Figure 8 shows a physical arrangement of the test setup. In addition to the sinusoidal test, the equipment compartment natural frequencies were excited by striking the vehicle at various locations and directions at station 52.05 with a rubber mallet. A comparison of the AVT-2 flight data, vibration survey data, and the AVT payload vibration flight-acceptance-test specification levels is given in table 4. The comparison indicates that resonant frequencies excited manually by mallet and those excited by the electromagnetic shakers were the same predominant frequencies determined from the PSD analyses of the flight vibration data. It may be remembered that similar predominant frequencies occurred during lift-off, MECO, fairing separation, and spacecraft separation.

Comparison With Pre-Flight Acceptance Test Levels

A comparison of the flight-measured values with the flight test specification (table 4) indicates that the previously written test specification is both adequate and not overly severe. The flight-measured overall level of 9.4 g-rms, at transonic speeds, is slightly below the test specification of 9.5 g-rms random excitation. However, since the predominant excitation occurred in the frequency band of 940 to 1,120 cps with an overall excitation level of 6.62 g-rms over this bandwidth (corresponds to a PSD of 0.488 g^2/cps), it is felt that the sinusoidal sweep at the level of 6 g-rms adequately simulates the flight vibration environment.

Effects of Nose Fairing Shapes

One of the effects of buffeting is the acoustical excitation of random vibrations in the vehicle and payload structures. Buffeting is usually defined as the result of unstable flow over the body and generally occurs as the vehicle approaches transonic speeds. The flow instability is essentially independent of body motions but is directly related to the vehicle nose shape. References 3, 4, and 5 report recent studies of buffeting forces on certain types of vehicle nose shapes. Figure 9 shows the nose shapes of three vehicles used to launch the S-51 (Thor-Delta), Transit BI (Thor-Able-Star), and AVT (Thor); from a study of the references it might be expected that the highest vibration levels due to buffeting would be measured on the Thor-Able-Star vehicle and the lowest on the Thor-Delta vehicle. Figure 10, which compares the overall rms flight vibration levels for these three vehicles[5], confirms that the vibration

[5]Thor-Able-Star data were obtained from reference 6 and Thor-Delta data from reference 2.

levels at transonic speeds were highest on the Thor-Able-Star and lowest on the Thor-Delta.

CONCLUDING REMARKS

The flight data presented in this report indicate that (1) the major vibration levels measured during the AVT flights occurred during lift-off, Mach 1, fairing separation, and payload separation; (2) the composite levels of both flights measured during these occurrences are in close agreement; (3) the spectra (level and frequency) are similar for comparative time data samples; and (4) the frequencies measured during flight were similar to those measured during the ground vibration survey.

Payload vibration data measured during a recent Thor-Delta flight show that no increase in level was measured during Mach 1 or maximum dynamic pressure; in contrast, high vibration levels were measured on the AVT flights. Also, high vibration levels were measured at Mach 1 and maximum dynamic pressure during flights of the Thor-Able-Star. The differences in the vibration levels of these vehicles measured at transonic speeds are attributed mainly to the vehicle nose shape.

A comparison of the flight-measured vibration levels with the environmental flight acceptance test specification indicates that the previously written test specification is both adequate and not overly severe.

REFERENCES

1. Tereniak, W. B., and Clevenson, S. A.: Flight Shock and Vibration Data of the ECHO A-12 Application Vertical Tests (AVT-1 and AVT-2). NASA TN D-1908, 1963

2. Williams, L. A.: Flight Vibration Data From the Delta 9 Launch Vehicle. NASA TN D-1683, 1963.

3. Woods, P., and Ericsson, L. E.: Aeroelastic Considerations in a Slender, Blunt-Nose, Multistage Rocket. Aerospace Eng. 21(5):42-51, May 1962.

4. Coe, C. F.: Steady and Fluctuating Pressures at Transonic Speeds on Two Space-Vehicle Payload Shapes. NASA TM X-503, 1961.

5. Coe, C. F.: The Effects of Some Variations in Launch-Vehicle Nose Shape on Steady and Fluctuating Pressures at Transonic Speeds. NASA TM X-646, 1962.

6. Douglas, D. G.: Measurement and Analysis of Missile Vibration, Shock, and Noise Environments. Proc. Instrum. Soc. Amer. 17(2): Paper No. 38.1.62, 1962.

Table 2

Summary of Predominant "High" Frequencies and Relative Vibratory Levels Measured on the AVT-1 and AVT-2 Principal Axes*

Liftoff				Main Engine Cutoff				Fairing Separation				Spacecraft Separation			
AVT-1		AVT-2		AVT-1		AVT-2		AVT-1		AVT-2		AVT-1		AVT-2	
Freq. (cps)	Level	Freq. (cps)	Level	Freq. (cps)	Level	Freq. (cps)	Level	Freq. (cps)	Level	Freq. (cps)	Level	Freq. (cps)	Level	Freq. (cps)	Level
Longitudinal Axis															
130	0.05	130	0.09	170	0.02	140	0.13	–	–	–	–	–	–	–	–
–	–	–	–	230	.02	280	.04	225	0.04	230	0.15	–	–	–	–
300	.05	330	.09	330	.02	340	.04	–	–	350	.19	–	–	350	0.10
430	.08	430	.32	380	.04	400	.03	420	.04	420	.24	410	0.08	440	.12
510	.12	–	–	480	.01	500	.02	–	–	480	.30	–	–	520	.12
585	.15	580	.49	570	.01	–	–	575	.11	570	.58	580	.08	580	.11
–	–	640	.60	620	.02	–	–	–	–	650	.33	–	–	670	.48
–	–	680	.51	700	.02	–	–	–	–	–	–	710	.13	–	–
760	.10	780	.41	750	.01	–	–	770	.08	780	.43	790	.23	–	–
–	–	–	–	800	.03	800	.01	–	–	–	–	–	–	800	.36
–	–	830	.35	850	.02	–	–	–	–	850	.52	840	.25	850	.48
890	.15	–	–	920	.02	–	–	910	.05	–	–	–	–	–	–
970	.11	960	.43	990	.01	950	.01	–	–	960	.86	–	–	–	–
1070	.19	1030	.57	–	–	1040	.01	1060	.09	1020	.24	1060	.26	1010	.55
1200	.11	1160	.31	1190	.40	–	–	1170	.04	1120	.29	–	–	–	–
–	–	1260	.25	–	–	1240	.01	1270	.04	–	–	1280	.09	1220	.26
1320	.09	1340	.16	1350	.01	–	–	–	–	–	–	1310	.09	1340	.21
1420	.08	–	–	–	–	–	–	1400	.08	1450	.22	1420	.09	–	–
–	–	1490	.27	–	–	–	–	1510	.05	–	–	1500	.09	1490	.14
1580	.07	1600	.05	–	–	–	–	–	–	–	–	–	–	–	–
1710	.04	1700	.05	–	–	–	–	–	–	1700	.11	–	–	–	–
–	–	1780	.10	–	–	–	–	1800	.02	–	–	1770	.06	1800	.07
Pitch Axis															
–	–	–	–	–	–	110	0.08	–	–	–	–	133	0.12	110	0.12
–	–	–	–	180	0.05	150	.07	–	–	–	–	–	–	170	.11
200	0.06	210	0.08	–	–	210	.05	220	0.20	220	0.22	210	.11	–	–
240	.09	260	.16	–	–	280	.03	–	–	260	.28	–	–	260	.08
310	.06	340	.10	330	.04	330	.07	340	.08	–	–	–	–	310	.09
–	–	–	–	380	.03	–	–	390	.10	360	.14	–	–	–	–
460	.09	470	.12	470	.02	–	–	440	.13	440	.10	440	.07	440	.09
–	–	540	.11	–	–	500	.02	550	.08	–	–	–	–	520	.05
–	–	–	–	580	.02	–	–	–	–	600	.17	–	–	620	.09
650	.06	640	.04	–	–	–	–	–	–	650	.15	650	.08	650	.07
–	–	700	.09	–	–	680	.01	–	–	–	–	–	–	–	–
–	–	–	–	740	.03	–	–	–	–	–	–	–	–	740	.04
–	–	790	.04	–	–	800	.01	780	.10	780	.14	810	.08	820	.11
830	.05	860	.10	860	.03	–	–	–	–	–	–	–	–	–	–
900	.05	–	–	–	–	–	–	920	.09	–	–	–	–	–	–
980	.04	970	.08	960	.04	–	–	–	–	–	–	990	.07	1000	.05
1050	.04	1030	.07	1030	.04	–	–	1060	.08	1030	.01	1060	.07	–	–
1100	.03	–	–	1080	.04	1100	.01	–	–	1100	.23	–	–	1100	.10
–	–	1160	.07	1170	.09	–	–	–	–	–	–	–	–	–	–
–	–	–	–	1210	.05	–	–	–	–	–	–	–	–	1220	.06
1290	.04	1260	.07	1205	.05	–	–	1260	.07	–	–	–	–	–	–
–	–	–	–	–	–	–	–	1340	.08	1370	.19	1350	.07	1340	.06
1440	.03	–	–	–	–	1470	.02	1500	.06	–	–	1480	.05	1460	.05
1650	.03	–	–	–	–	–	–	1680	.06	1650	.12	1640	.06	1650	.06
–	–	1810	.04	–	–	1880	.02	1800	.05	1850	.06	1830	.05	1850	.04
Yaw Axis															
–	–	130	0.05	–	–	140	0.04	170	0.17	–	–	140	0.12	130	0.18
220	0.12	–	–	180	0.09	200	.03	210	.39	–	–	200	.12	–	–
260	.10	230	.13	–	–	–	–	–	–	250	0.04	250	.07	250	.18
–	–	300	.14	–	–	270	.02	280	.08	–	–	280	.07	–	–
–	–	350	.18	330	.11	330	.05	320	.09	340	.03	320	.05	340	.24
–	–	–	–	–	–	–	–	420	.14	420	.03	410	.04	430	.12
440	.09	–	–	450	.06	–	–	450	.08	460	.02	–	–	–	–
490	.07	480	.12	500	.08	–	–	–	–	530	.02	520	.04	–	–
–	–	600	.10	620	.09	600	.01	560	.05	600	.02	–	–	620	.09
650	.05	–	–	680	.09	–	–	–	–	670	.02	650	.04	670	.10
780	.05	770	.07	750	.10	–	–	770	.06	–	–	–	–	780	.06
820	.05	–	–	–	–	800	.01	–	–	800	.01	810	.03	–	–
–	–	840	.07	850	.12	–	–	830	.05	850	.02	850	.03	–	–
980	.04	–	–	950	.12	–	–	–	–	–	–	–	–	–	–
–	–	1000	.04	1000	.10	–	–	–	–	–	–	–	–	–	–
1040	.03	1080	.03	–	–	1070	.01	–	–	1030	.01	–	–	1030	.04
–	–	–	–	1120	.10	–	–	–	–	–	–	–	–	–	–
–	–	–	–	1160	.19	–	–	–	–	–	–	–	–	–	–
–	–	1270	.02	1280	.08	–	–	–	–	–	–	–	–	1280	.02
–	–	1380	.01	1390	.07	–	–	–	–	–	–	–	–	–	–
–	–	1740	.01	–	–	–	–	–	–	–	–	–	–	–	–

*All levels are relative; analysis filter bandwidth, 20 cps.

Table 3

Summary of AVT Low Frequencies at Their Maximum Level.

Longitudinal Axis				Pitch Axis				Yaw Axis*			
AVT-1		AVT-2		AVT-1		AVT-2		AVT-1		AVT-2	
Freq. (cps)	Level (g-pk)	Freq. (cps)	Level (g-pk)	Freq. (cps)	Level (g-pk)	Freq. (cps)	Level (g-pk)	Freq. (cps)	Level (g-pk)	Freq. (cps)	Level (g-pk)
Liftoff											
17	1.8	17	1.0	8	0.70	8	0.5	11	1.4	11	1.1
22	2.0	–	–	–	–	9	.80	22	.70	–	–
33	1.6	–	–	–	–	11	1.0	33	.50	–	–
44	1.3	45	1.0	22	.40	–	–	–	–	45	.30
57	1.8	–	–	33	.40	–	–	57	.70	–	–
–	–	–	–	–	–	45	.90	–	–	–	–
–	–	–	–	57	.80	–	–	–	–	–	–
Main Engine Cutoff											
–	–	32	0.76	–	–	52	0.3				
–	–	42	.65	–	–	58	1.1				
55	0.4	55	.65	87	0.69	–	–				
95	.2	–	–	116	.87	–	–				
122	.91	–	–								
–	–	137	2.8								

*Yaw axis has no significant levels in the 5-150 cps range during main engine cutoff.

Table 4

Comparison of Flight Vibration Data with Ground Vibration Survey Frequencies and Test Specification Levels*

Ground Vibration Data, Thrust			AVT-2 Flight Vibration Data, Power Spectral Density*				Flight Test Levels, Sinusoidal	
Tapping	Forced Vibration							
Freq. (cps)	Freq. (cps)	Response (± g)	Freq. (cps)	Yaw (g^2/cps†)	Pitch (g^2/cps‡)	Thrust (g^2/cps**)	Freq. Range (cps)	Level
210	–	–	–	–	–	–	5–14	$\frac{1}{4}$ inch D. A.
400	390	3.3	340	0.0171	0.0071	–	14–400	4 g-rms
435	490	5.8	470	.0169	.0098	0.02	400–2000	6 g-rms
–	585	4.6	575–625	.0114	.0065	.102		
–	–	–	675–710	.0168	.0088	.058		
–	795	5.3	775–825	.0148	.0076	.024		
915	915	8.3	900	–	–	.028		
–	970	8.8	950	–	–	.102		
–	1040	10	1030	.0098	.0066	.488		
1100	1120	7.4	1100	.0133	.0062	.066		
1180	–	–	1180	–	–	.069		
1250	1200	6.4	1220	.0060	.0063	.065		
–	–	–	1280	–	–	.035		
–	–	–	1320	–	.0012	.032		
–	–	–	1380	–	–	.033		
–	–	–	1440	–	–	.026		
1570	1550	5.7	1500	–	.014	.029		
–	–	–	1630	–	.0067	–		
							Gaussian Random	
							15–2000 cps	0.045 g^2/cps (9.5 g-rms)

*Data sample measured at maximum flight vibration level, T+38 to T+40 seconds.
†Filter bandwidth, 50 cps.
‡Filter bandwidth, 50 cps.
**Filter bandwidth, 20 cps.

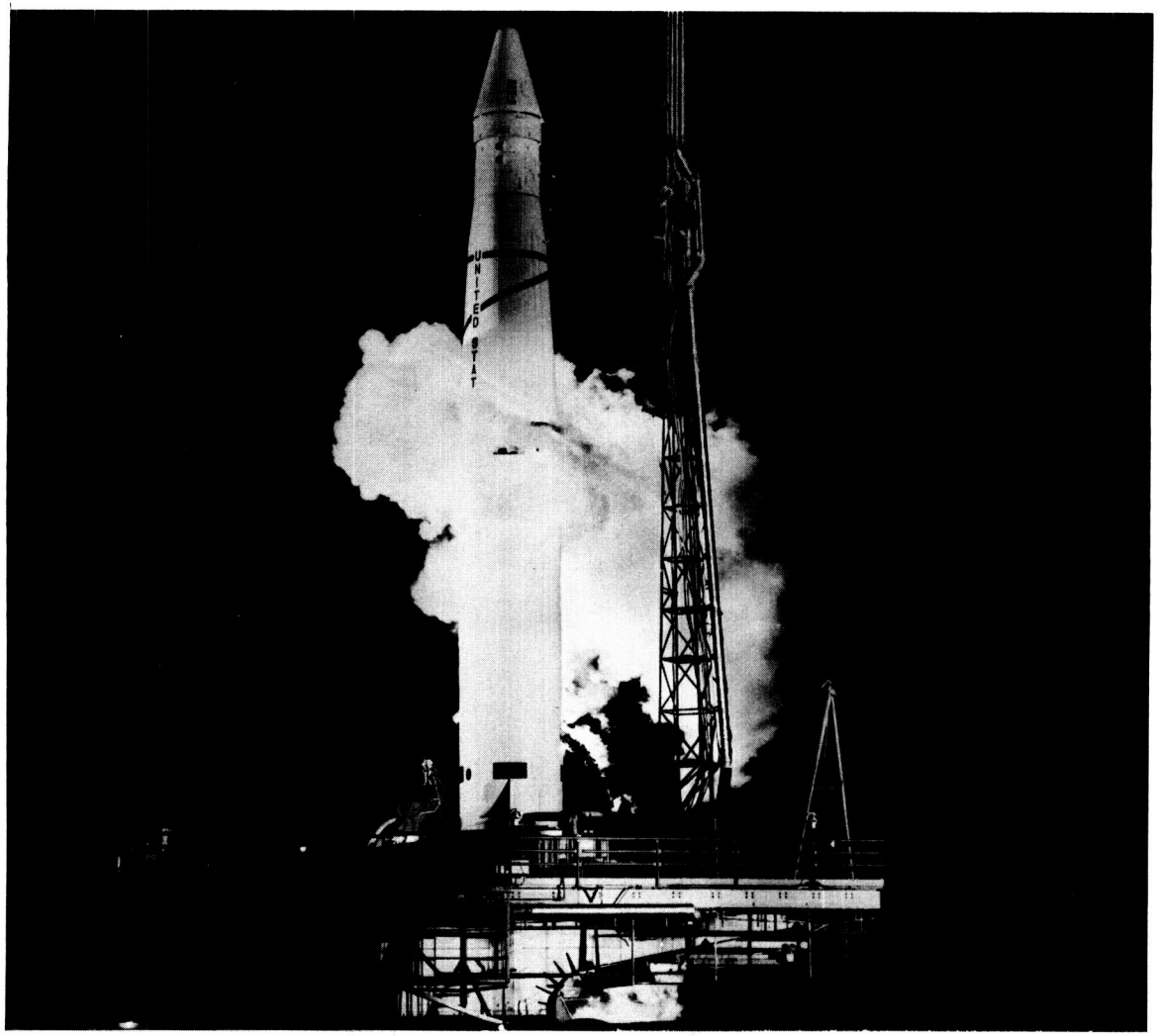

NASA

Figure 1.- AVT vehicle on launch pad at AMR.

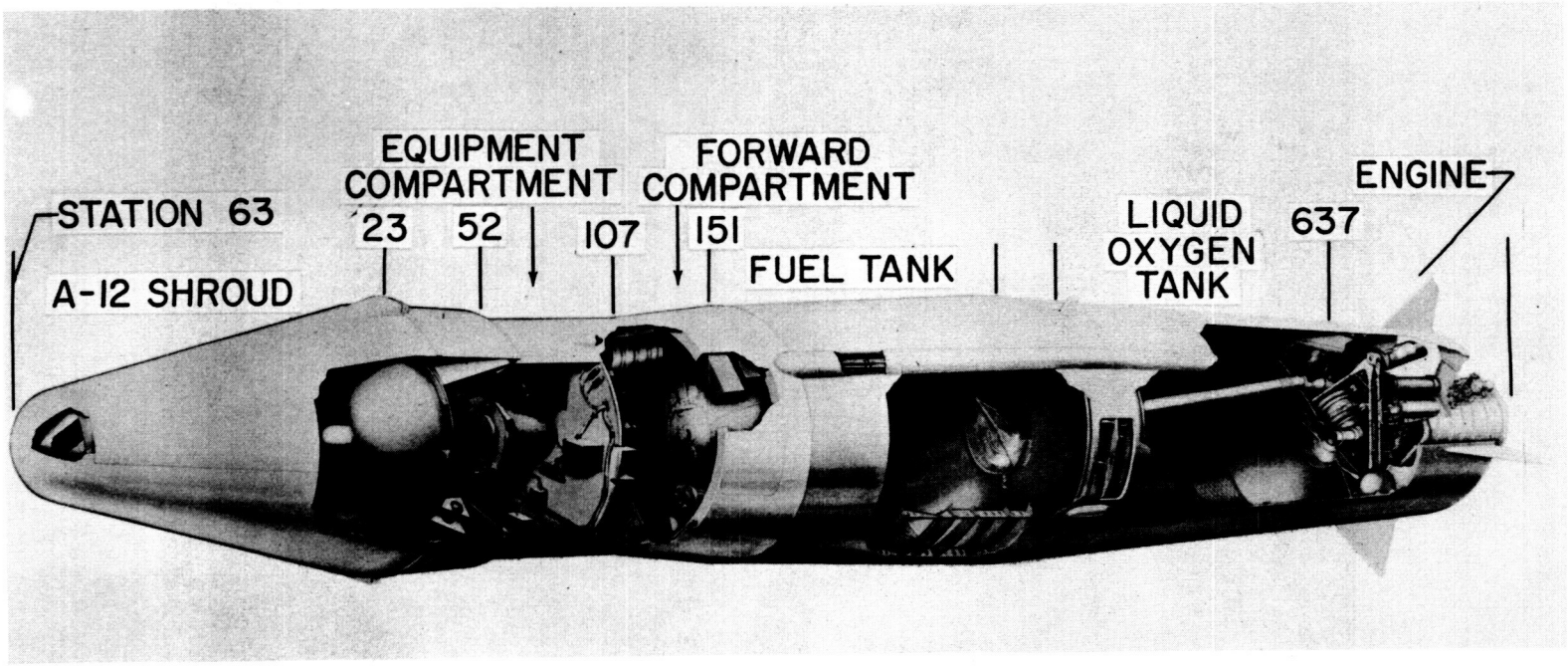

NASA

Figure 2.- Cutaway view of AVT vehicle.

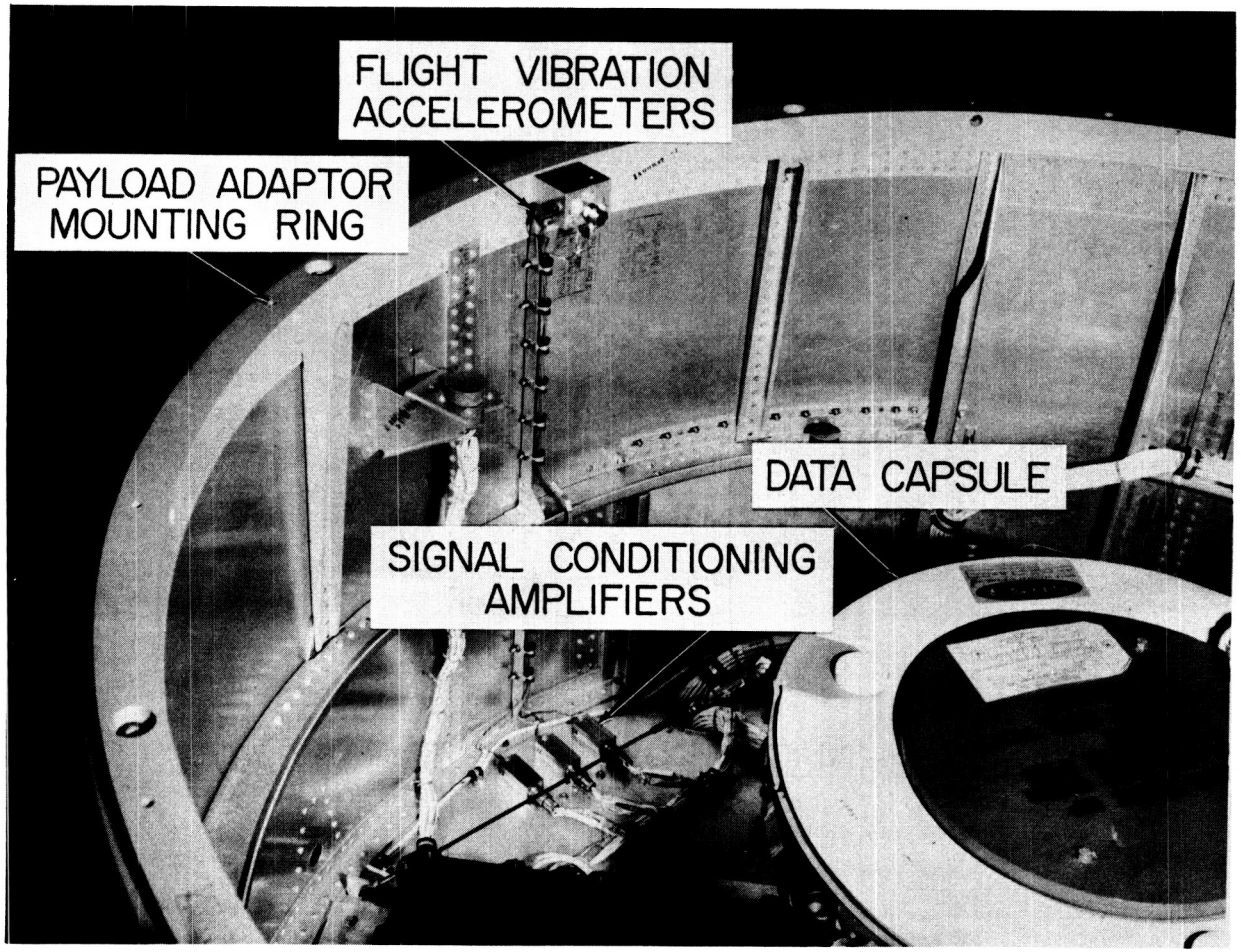

NASA

Figure 3.- Instrumentation in equipment compartment.

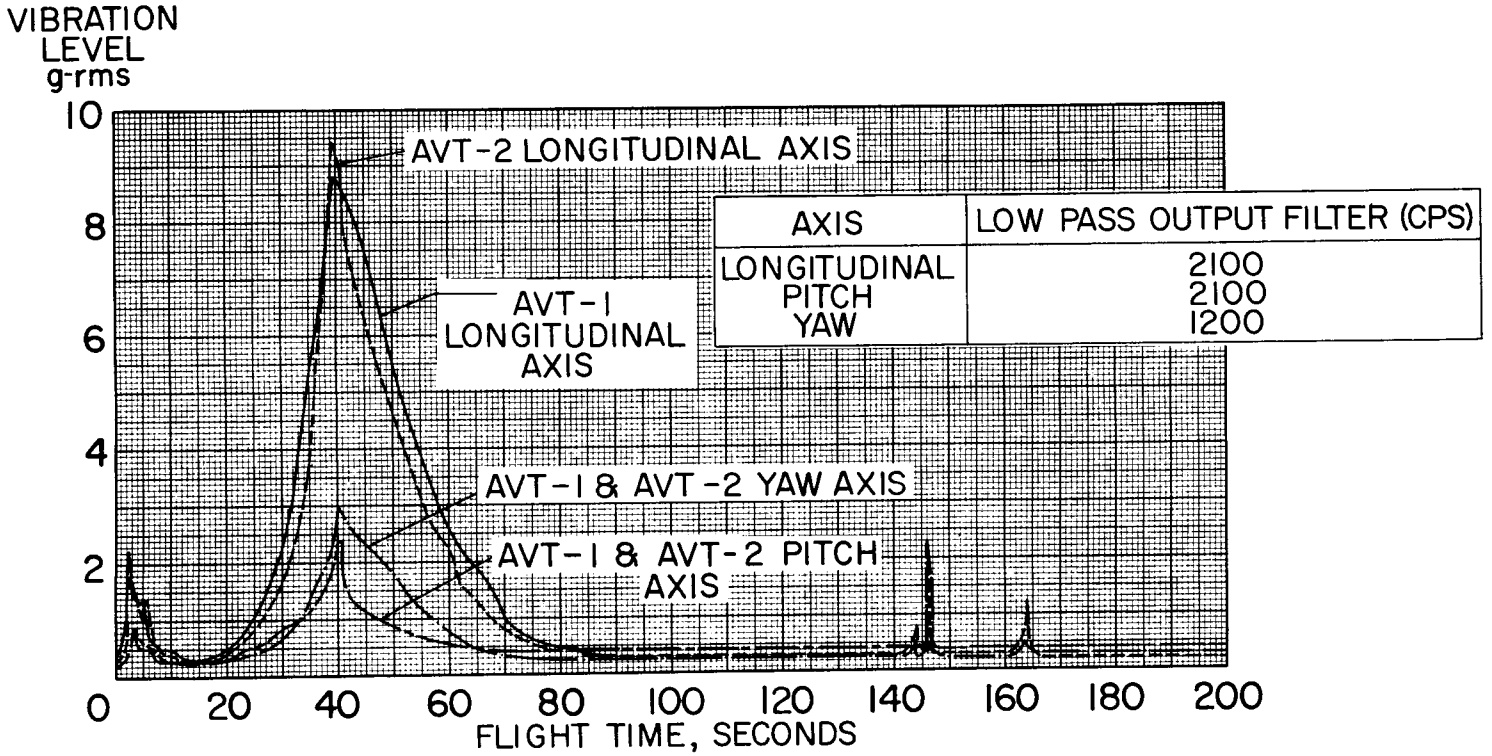

NASA

Figure 4.- Overall in-flight vibrations - AVT 1 and 2.

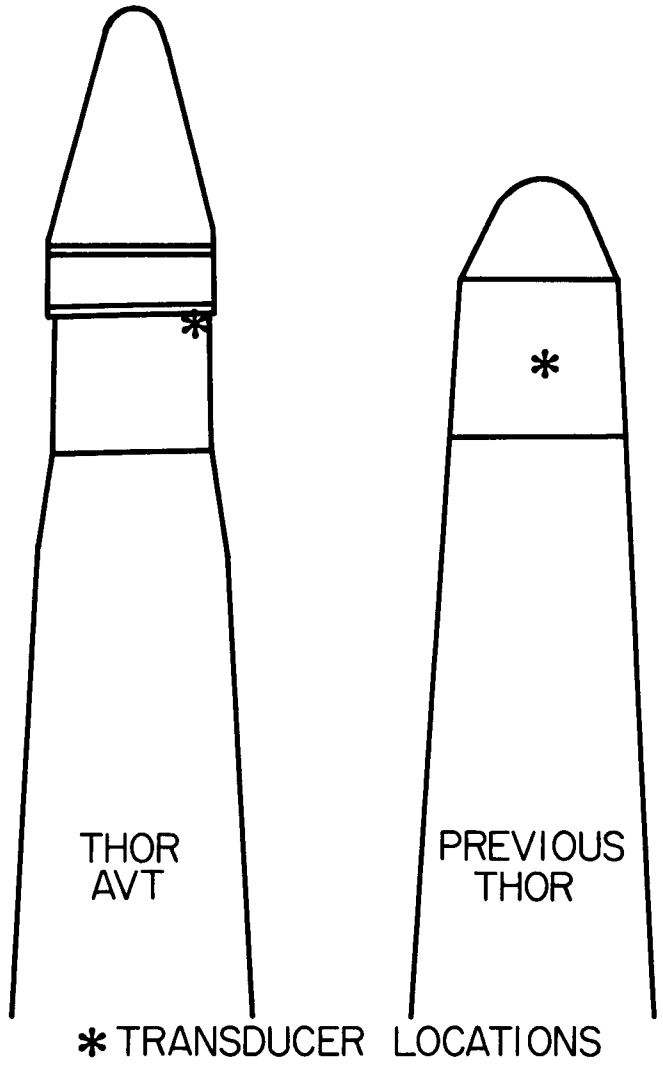

NASA

Figure 5.- Comparison of AVT and previous THOR nose shapes and locations of the vibration transducers.

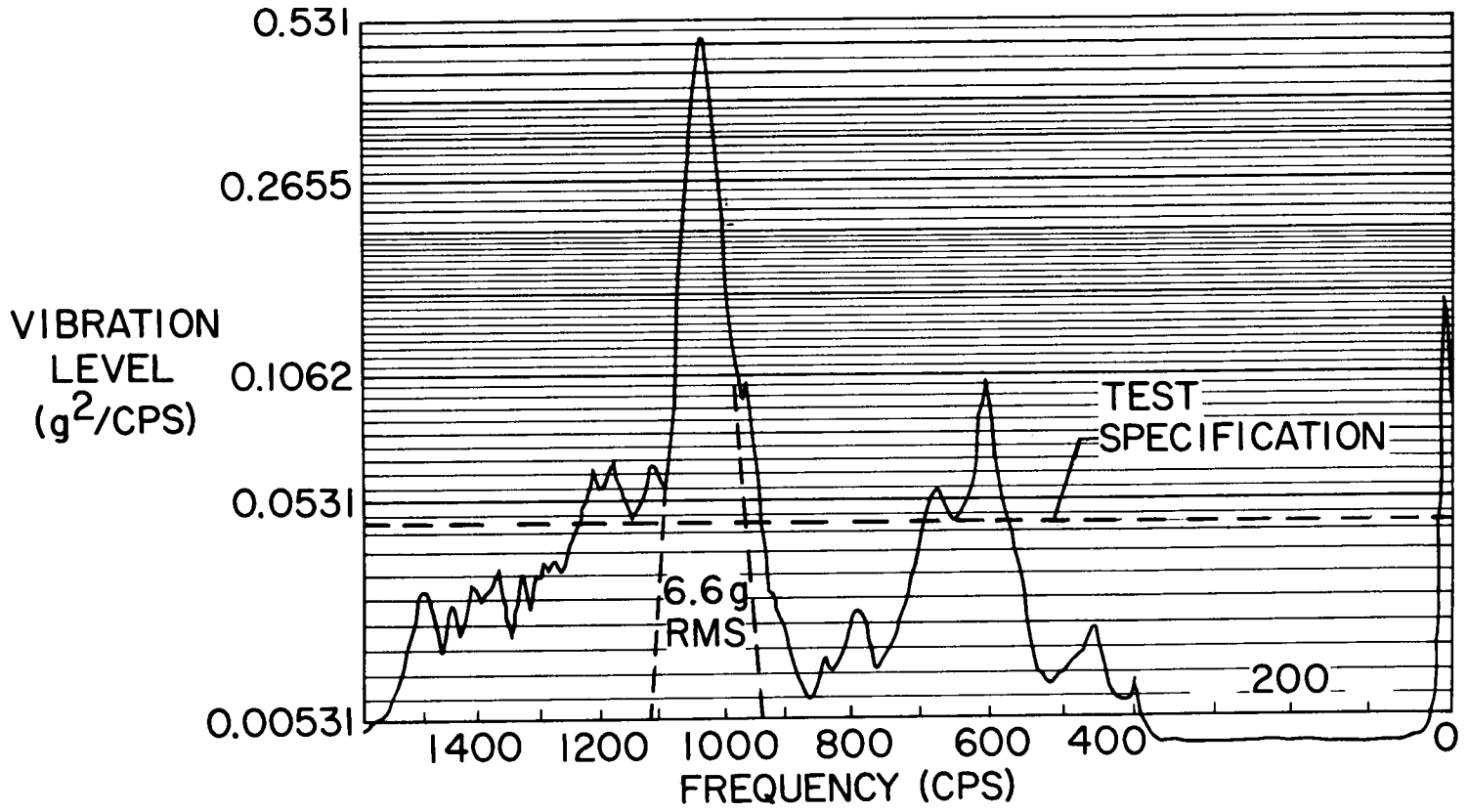

NASA

Figure 6.- PSD of longitudinal vibration at M = 1 (t = 38-40 sec). Filter bandwidth, 20 cps; RC averaging time, 1 sec; sample length, 2 sec.

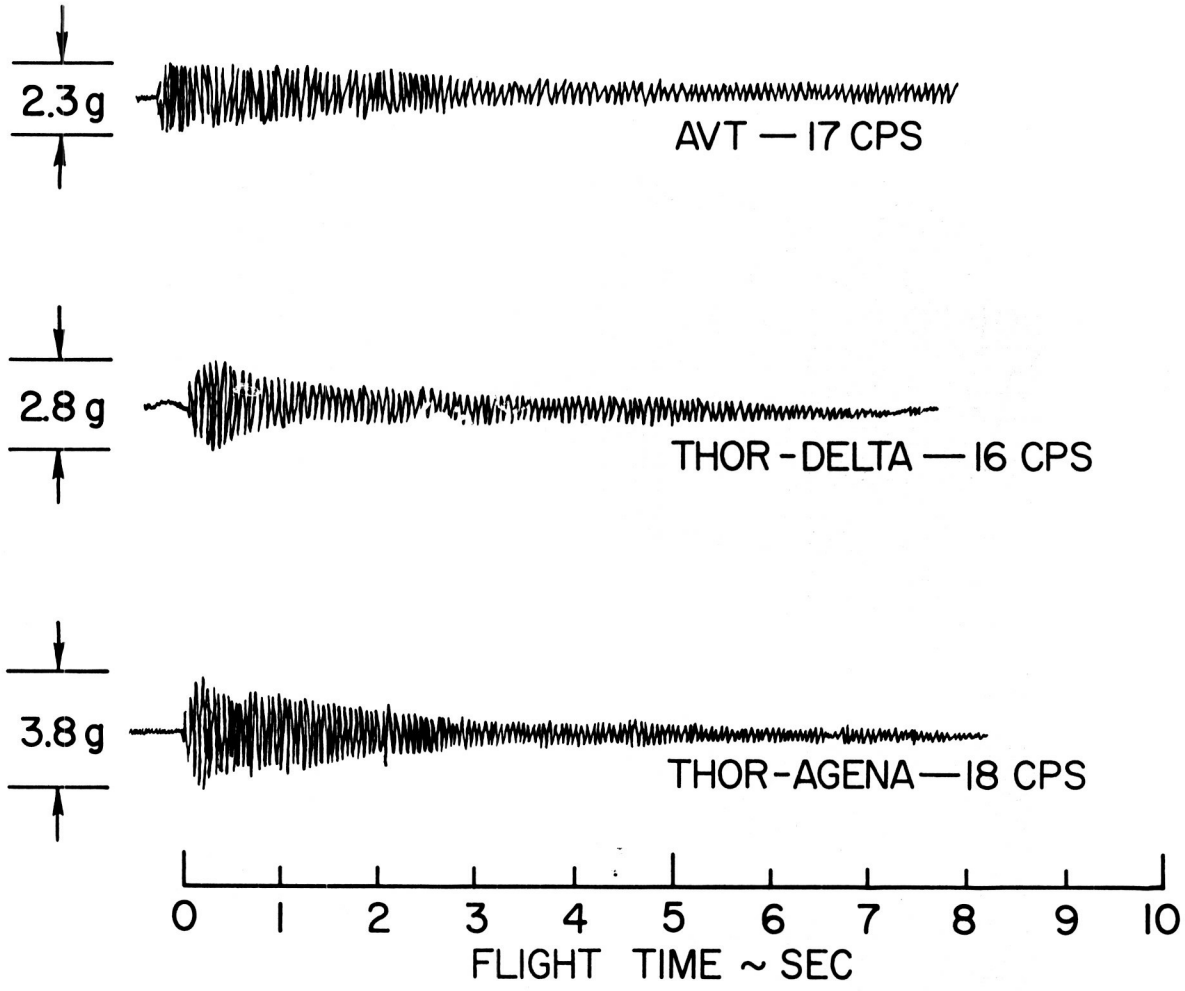

NASA

Figure 7.- Discreet frequencies measured at lift-off on the AVT, Thor-Delta, and Thor-Agena vehicles. Narrow bandpass filters used.

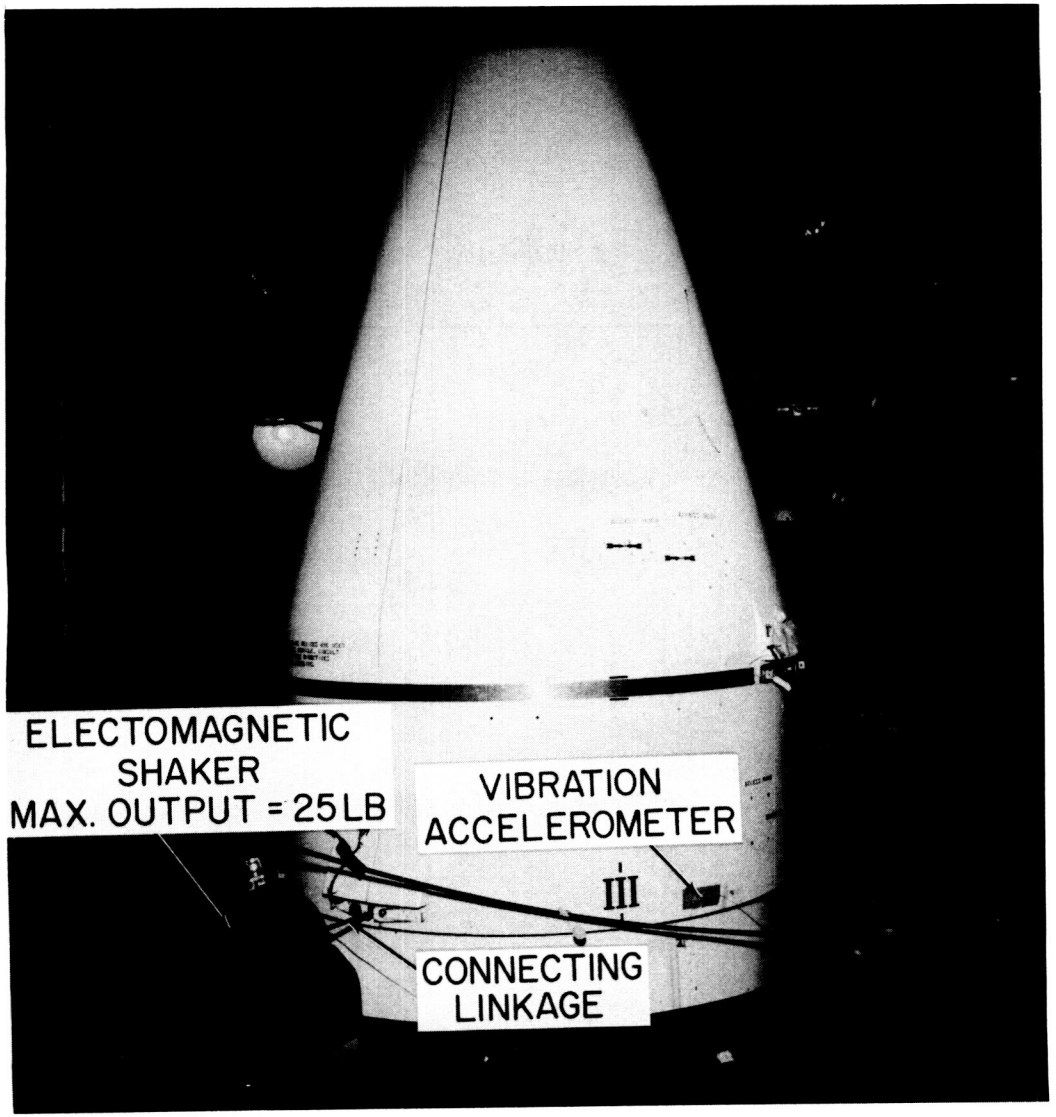

NASA

Figure 8.- Equipment arrangement for vibration survey.

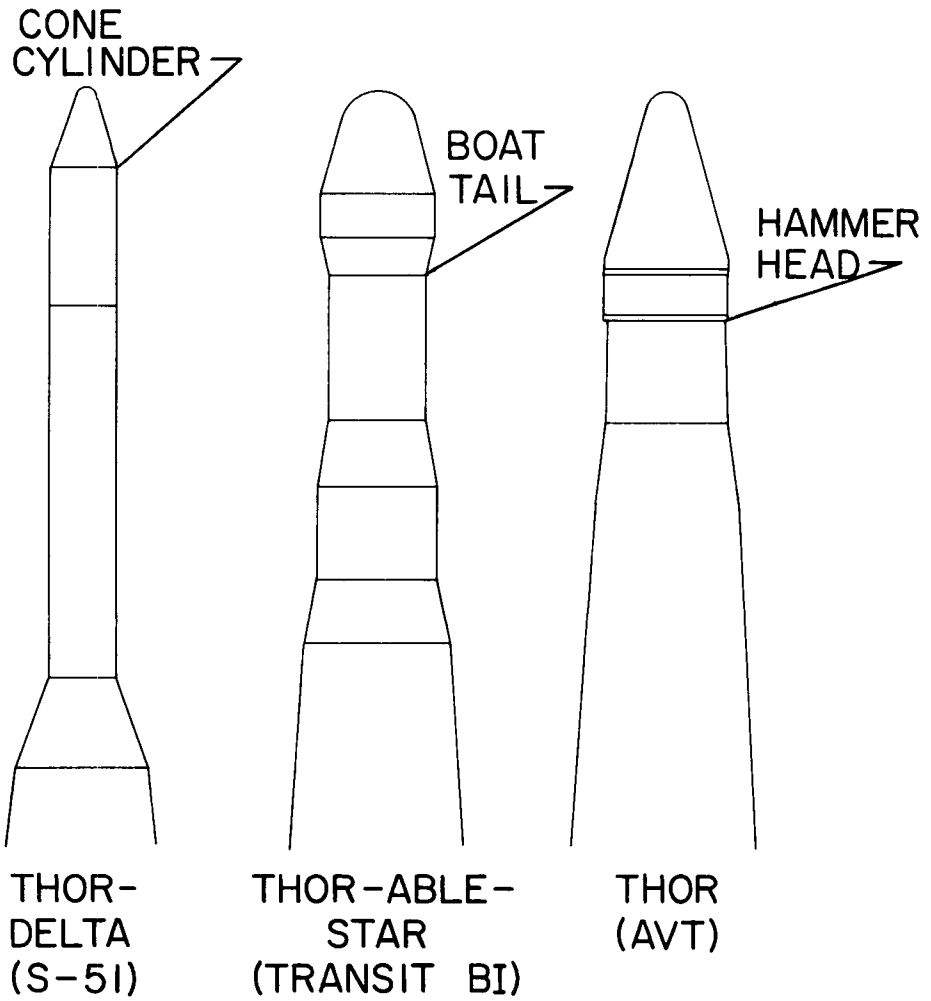

NASA

Figure 9.- Comparison of Thor-Delta, Thor-Able-Star, and AVT nose shapes.

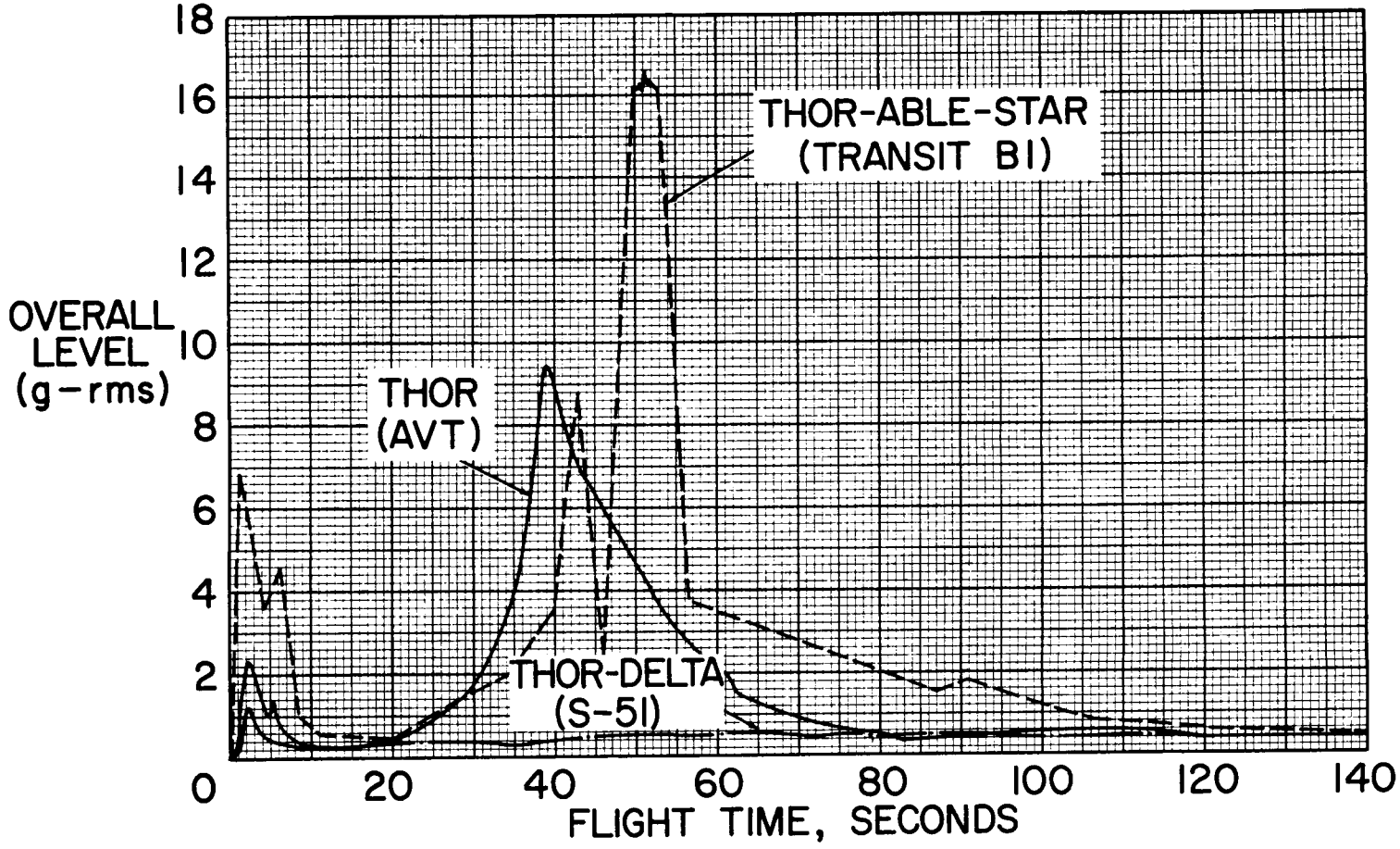

Figure 10.- Longitudinal vibration-time history comparison of AVT, Thor-Delta, and Thor-Able-Star flights.

NASA-Langley, 1963